Research Square

Preprints are preliminary reports that have not undergone peer review.
They should not be considered conclusive, used to inform clinical practice,
or referenced by the media as validated information.

Systems-level transcriptomics reveals the regulatory architecture of the post-pollination syndrome in Vanilla planifolia

Olga Andrea Hernández-Miranda
andii_93manch@comunidad.unam.mx
Universidad Nacional Autónoma de México
Jorge E. Campos
Universidad Nacional Autónoma de México
Ulises Rosas
Universidad Nacional Autónoma de México
Estela Sandoval-Zapotitla
Universidad Nacional Autónoma de México
Ana Sidney Betanzos Ávalos
Universidad Nacional Autónoma de México
Juan Alberto Villanueva García
Universidad Nacional Autónoma de México
María Concepción Guzmán Ramos
Universidad Nacional Autónoma de México
Victor Manuel Salazar-Rojas
Universidad Nacional Autónoma de México

Research Article

Keywords: Post-pollination syndrome, phytohormone signaling, systems biology, vanilla, orthology inference, transcriptomics

Posted Date: September 28th, 2026

DOI: https://doi.org/10.21203/rs.3.rs-11022553/v1

License: This work is licensed under a Creative Commons Attribution 4.0 International License.
Read Full License

Additional Declarations: No competing interests reported.

Abstract

In many angiosperms, reproductive development depends on pollination-induced reprogramming of ovary and ovule growth; however, the mechanisms coordinating this development remain poorly understood, particularly in non-model species. In orchids such as *Vanilla planifolia* Andrews, this process involves a distinctive post-pollination syndrome in which ovule development is reactivated following pollination and proceeds through a prolonged, environmentally responsive developmental program. To characterize the organization of this syndrome, we integrated developmental anatomical analyses with systems-level transcriptomics, combining orthology inference, differential expression analysis, co-expression network reconstruction, and a bioinformatic labeling framework that encompasses structural and functional dimensions of gene regulation. Co-expression analysis identified nine transcriptional modules associated with reproductive development, metabolism, chromatin organization, and gene expression regulation, with enrichment in hormone signaling pathways. By intersecting structural and functional labels, we prioritized 88 candidate regulators associated with the post-pollination syndrome and classified them according to their roles within the architecture and function of the system. Our results define a molecular framework for the post-pollination syndrome and the flower-to-fruit transition in *Vanilla planifolia*, linking transcriptional organization with anatomical development and supporting its interpretation as an integrated regulatory system. This approach provides a reproducible and generalizable strategy for identifying and prioritizing key regulators in non-model plants with complex reproductive transitions.

Key message

Nine regulatory modules and 88 prioritized candidate regulators define a molecular framework linking transcriptional organization with anatomical development during pollination-dependent reproductive development in orchids.

Introduction

The flower-to-fruit transition (FFT) is a fundamental developmental process that determines reproductive success in angiosperms and has been extensively characterized in model species such as *Arabidopsis thaliana* L. (Brassicaceae) (Lord et al. 2002; Chevalier et al. 2011). In most species, ovule development and fruit initiation occur continuously. However, in several lineages, including orchids, reproductive development follows a variant in which ovule and ovary growth are activated only after pollination. This phenomenon, known as the post-pollination syndrome (PPS), involves a delayed developmental program in which female gametophyte formation, ovule maturation, and fruit initiation depend on pollination-derived signals (O'Neill 1997), suggesting the presence of an integrated regulatory network coordinating these processes.

In *Vanilla planifolia* Andrews (Orchidaceae), a tropical crop of high economic value, the post-pollination phase can extend for several months. During this period, ovule differentiation, fertilization, and early fruit

development take place while the plant integrates environmental cues. Fluctuations during this interval can trigger stress responses, disrupt fertilization, and lead to ovary abscission, thereby affecting reproductive success and yield (Ruan et al. 2012; Salazar-Rojas et al. 2016; Hernández-Miranda et al. 2020). Despite its biological and agricultural importance, the regulatory organization underlying this pollination-dependent transition, particularly in terms of co-expression modules and key genes, remains poorly understood (O'Neill 1997; Levine et al. 2005; Pajoro et al. 2014).

An additional challenge is that many key events occur at the tissue level and cannot be detected through external morphological observations (O'Neill 1997; Lord et al. 2002). In this context, anatomical characterization of the ovary establishes the tissue-level framework of development (Endress 2011), facilitating the interpretation of transcriptional dynamics and providing critical biological context for integrative analyses (Kudoh 2016; Tornielli et al. 2023).

Within this framework, systems-level developmental transcriptomics emerges as a data-driven approach to describe the regulatory organization of complex processes by modeling gene expression as coordinated networks rather than isolated responses. From this perspective, the FFT can be understood as a complex biological system in which multiple regulatory layers interact dynamically (Kitano 2002; Barabási et al. 2004), enabling the identification of co-expression modules and candidate genes associated with integrated developmental programs (Busser et al. 2008). Previous studies have shown that this analytical framework can reveal transcriptional modules involved in reproductive development across plant systems. For example, co-expression network analysis in *Fragaria vesca* L. (Rosaceae) identified modules associated with anthesis and pollination (Shahan et al. 2018), while comparative studies in Solanaceae species revealed conserved regulatory architectures underlying flower and fruit development (Zhang et al. 2025). Similarly, the integration of transcriptomic networks with functional annotation and evolutionary conservation has enabled the prioritization of regulatory genes associated with coordinated developmental processes, as demonstrated in studies of seed development in *Arachis hypogaea* L. (Fabaceae) (Yang et al. 2023).

In *V. planifolia*, our previous study defined four molecular phenological stages associated with the PPS and revealed extensive transcriptional reprogramming (Hernández-Miranda et al. 2025). However, the regulatory organization of this process in terms of co-expression networks, functional modules, and key genes underlying the FFT under this syndrome remains unknown. Based on this framework, the aim of this study was to characterize the regulatory organization of the PPS during the FFT in *V. planifolia* using a systems-level transcriptomic approach (Hernández-Miranda et al. 2025). To this end, we developed a reproducible workflow integrating transcriptomic data, anatomical context, and functional annotation, together with a structural and functional network labeling scheme, enabling analysis across multiple regulatory dimensions. This approach not only describes transcriptome organization but also provides a reproducible and transferable analytical framework for the identification of candidate genes associated with complex developmental processes in non-model species.

Materials and Methods

Data Description

We used our previously assembled and annotated transcriptome of the FFT in *V. planifolia*, comprising four molecular phenological stages: (1) pre-pollination (Pre-pol; floral bud prior to anthesis), (2) pollination (Pol; flower at anthesis with pollen deposited on the stigma), (3) post-pollination (Post-pol; ovary 25 days after pollination), and (4) fertilization (Fer; ovary with fertilized ovules, 60 days after pollination) (Hernández-Miranda et al. 2025). Raw sequencing data are available under BioProject PRJNA808623, and the assembled and annotated transcriptome is available at Zenodo (https://doi.org/10.5281/zenodo.18916399; https://doi.org/10.5281/zenodo.18765805).

We further incorporated publicly available transcriptomic datasets from *A. thaliana*, *Solanum lycopersicum* L. (Solanaceae), *Vitis vinifera* L. (Vitaceae), and *V. planifolia*, associated with floral development and the flower-to-fruit transition, obtained from Ensembl Plants (Table S1) (Bolser et al. 2016). Differentially expressed gene (DEG) datasets from these species were compiled into a unified dataset, available at Zenodo (https://doi.org/10.5281/zenodo.18795437).

Anatomical analysis

In order to understand the development patterns during the four phenological stages, gynostemium samples were taken in each of them. The gynostemium was subdivided into apical, medial, and basal regions, and samples were also collected from the medial region of the ovary. Tissues were fixed in formaldehyde–alcohol–acetic acid (FAA; 10% formaldehyde, 50% ethanol, 5% acetic acid, 35% distilled water) for 24 h, rinsed with distilled water, and softened in 10% ethylenediamine for an additional 24 h prior to dehydration. Dehydration was performed through a graded tert-butyl alcohol series (30%, 50%, 60%, 75%, 80%, 90%, 100%, and absolute). Samples were infiltrated and embedded in Paraplast (Sigma-Aldrich) and methacrylate resin (Leica) (Sandoval-Zapotitla et al. 2005). Longitudinal sections of the gynostemium and transverse sections of the ovary were obtained at 5 µm thickness using a rotary microtome (American Optical model 820). Sections were stained with safranin and fast green and mounted with synthetic resin (Sandoval-Zapotitla et al. 2005). Histological slides were deposited in the collection of the Laboratorio de Apoyo a la Investigación, Jardín Botánico, Instituto de Biología, Universidad Nacional Autónoma de México. Samples were examined using a photomicroscope (Carl Zeiss Axioskop) equipped with bright-field, phase-contrast, and polarized-light optics. Dermal, ground, and vascular tissues of the gynostemium and ovary/fruit were analyzed, and images were captured using a digital camera (RisingView V x64.4.10.17214.2020).

Generation of functional and structural labels for the flower-to-fruit transition transcriptome in *Vanilla planifolia*

As outlined in the workflow shown in Fig. 1, we generated a set of structural and functional labels to analyze transcriptional dynamics during the FFT using custom scripts implemented in R (v4.2.3) and Perl (v5.28.1). These labels were designed to capture biologically relevant dimensions of gene regulation,

including evolutionary conservation, developmental specificity, regulatory potential, and network centrality.

Functional labels

Conserved ortholog label (C-Orth):

To generate this label, we selected published transcriptomes associated with floral development (FD) and the FFT from angiosperms with curated genomes available in Ensembl Plants (*A. thaliana*, *S. lycopersicum*, and *V. vinifera*) (Table S1) (Bolser et al. 2017). DEG lists were compiled for these species and for *V. planifolia* (Supplementary Fig. S1) (data available at: https://doi.org/10.5281/zenodo.18795437). Gene sequences were retrieved using Perl (v5.28.1) scripts (available at: https://github.com/Andrea-H-M/SystemsLevel_transcriptomics/tree/main/C_Orth_label).

Orthology inference was performed using OrthoFinder (v 2.5.5) (Emms et al. 2019), and orthogroups shared among the four species were filtered using custom scripts in R (v4.2.3) to identify conserved orthologs (C-Orth) associated with the flower-to-fruit transition (Supplementary Fig. S2).

Functional enrichment analysis was conducted using Planteome and Gene Ontology (GO) (accessed in 2023), with *A. thaliana* as the reference species (Cooper et al. 2024). Enriched terms ($p \leq 0.05$) were visualized using bubble plots, and gene family classifications were represented using bar plots in R (v4.2.3) (Fig. 1; Supplementary Fig. S3).

Stage-associated gene labels (Pre-pol, Pol, Post-pol, and Fer):

To define this label, functional signatures associated with stage-associated development were extracted from the FFT transcriptome of *V. planifolia*. These correspond to genes showing significantly higher expression in one stage compared with the others ($p \leq 0.00001$) (data available at: https://zenodo.org/records/18765805) (Hernández-Miranda et al. 2025) (Fig. 1).

Transcription factor (TF) and epigenetic regulator (EpiReg) labels:

To generate transcription factor (TF) and epigenetic regulators (EpiReg) labels, TF identifiers for *A. thaliana* were retrieved from PlantTFDB v5 (Jin et al. 2017). Epigenetic regulators were identified based on curated functional domains associated no with histone modification, chromatin remodeling, epigenetic readers, and DNA methylation, obtained through targeted searches in PLAZA v5.0 (Van Bel et al. 2022). A unified list of TF and EpiReg identifiers was used to retrieve InterPro/PFAM domain annotations in PLAZA v5.0, which were subsequently used to query the *V. planifolia* transcriptome using custom scripts implemented in Perl v5.28.1 (Hernández-Miranda et al. 2025) (scripts available at: https://github.com/Andrea-H-M/SystemsLevel_transcriptomics/tree/main/TF_EpiReg_labels). Functional enrichment analysis of TF and EpiReg gene sets was performed using gProfiler (accessed in 2025) with GO categories, using *A. thaliana* as the reference organism. Enriched terms were visualized using bubble plots and bar charts (Fig. 1; Supplementary Figs. S4, S5) (Raudvere et al. 2019).

Structural label generation

Differentially expressed gene (DEG) label:

To define this label, transcripts showing significant differential expression (log_2 fold change ≥ 2 and $p \leq 0.00001$) across developmental stages (Pre-pol, Pol, Post-pol, and Fer) were extracted from the FFT transcriptome of *V. planifolia* (data available at: https://zenodo.org/records/18765805) (Hernández-Miranda et al. 2025) (Fig. 1).

Module hub genes (Hub):

To generate the module hub gene (Hub) label, variance-based filtering was applied while retaining TF and EpiReg. Genes were ranked by expression variance, and those up to the inflection point of the cumulative variance curve were selected (Supplementary Fig. S6). Gene co-expression networks were constructed using weighted gene co-expression network analysis (WGCNA) in R v4.2.3 from normalized transcriptomic data. Modules were identified using dynamic tree cutting and subsequently merged based on eigengene correlation (cutHeight = 0.4), achieving high mean module compactness (>0.85) (Supplementary Fig. S7) (Langfelder et al. 2008). Functional enrichment analysis was performed using GO categories in gProfiler and Kyoto Encyclopedia of Genes and Genomes (KEGG) metabolic pathways (accessed in 2025) (Supplementary Figs. S8–S10) (Kanehisa et al. 2000; Raudvere et al. 2019). Hub genes within each module were defined based on high intramodular connectivity, using thresholds of module membership (MM) > 0.8 and kWithin ≥ 90th percentile (scripts available at: https://github.com/Andrea-H-M/SystemsLevel_transcriptomics/tree/main/Hub_label) (Supplementary Figs. S11–S14) (Kanehisa et al. 2000; Langfelder et al. 2008; Liu et al. 2019; Feng et al. 2021) (Fig. 1).

Integration of transcriptional labels and network topology for candidate gene prioritization:

Combinations of transcriptional labels within the transcriptome were analyzed using an UpSet plot generated in R v4.2.3 (Lex et al. 2014). These labels were subsequently integrated into the topological overlap matrix (TOM) to construct gene co-expression networks, which were visualized as pie-chart nodes using the igraph package in R v4.2.3, enabling the representation of label composition within each module (Pavlopoulos et al. 2015). To prioritize candidate genes associated with the functional and structural dynamics of the FFT, a classification framework integrating functional labels (C-Orth, Pol, Post-pol, Fer, TF, and EpiReg) and structural labels (DEG and Hub) was applied. Genes carrying both label types were selected as candidate regulators (scripts available at: https://github.com/Andrea-H-M/SystemsLevel_transcriptomics/tree/main/Candidate_genes_priorization) (Aerts et al. 2006; Langfelder et al. 2008; Zhang et al. 2005) (Fig. 1). The resulting dataset is publicly available at: https://doi.org/10.5281/zenodo.18795618

Results

Anatomical context of the post-pollination syndrome during the flower-to-fruit transition in *Vanilla planifolia*

Anatomical analysis was performed to define the developmental context of the FFT in *V. planifolia*, describing the sequence of ovary activation and tissue differentiation. This framework enabled the interpretation of the co-expression network across developmental stages and supported the prioritization of candidate genes associated with the overall FFT process:

Pre-pollination stage (final floral morphogenesis and flower maturation)

The ovary consists of three fused carpels forming a single locule and is lined by a uniseriate epidermis, each carpel includes several major collateral vascular bundles located centrally (Fig. 2a). Placental ridges differentiate from the inner epidermal cells and proliferate into nucellar filaments (placental projections) adjacent to minor vascular bundles (Fig. 2b). These filaments comprise a single axial row of cells surrounded by an epidermal layer with conspicuous, chromatin-rich nuclei (Fig. 2c).

Pollination stage (pollen tube growth and initiation of megasporogenesis)

The ovarian cavity exhibits proliferating placental projections with dense nuclei in distal cells, alongside differentiation of the transmitting tissue. Pollen tubes germinate within the receptive stigmatic cavity and grow toward the ovary (Fig. 2d). Ovule development initiates from nucellar filaments as the terminal cell enlarges and differentiates into the archesporial cell (megasporocyte). The inner integument forms a two-layered structure surrounding the developing embryo sac and defining the micropyle, while the outer integument begins to develop. At the funiculus, cell divisions and curvature establish an anatropous ovule with defined chalazal and micropylar regions (Fig. 2e–f).

Post-pollination stage (megagametogenesis and embryo sac development)

The functional megaspore at the chalazal end undergoes mitotic divisions to form the embryo sac, which contains six nuclei: two antipodals, two synergids, one egg cell, and one central nucleus (Fig. 2g). Concurrently, the initiation of the embryo with suspensory is observed, the nucellus and inner integument are reduced, while the outer integument encloses the ovule. Seed coat formation initiates through thickening of anticlinal walls in the outer layer of the outer integument (Fig. 2h).

Fertilization stage (fertilization and early embryogenesis)

Following fertilization, embryo differentiation and seed coat formation are continued, with the latter derived from the outermost layer of the outer integument. Glandular trichomes are observed on the inner ovary wall (Fig. 2i). This is accompanied by progressive degeneration of nucellar tissue and the emergence of suspensor-forming cells (Fig. 2j). Developing seeds subsequently contain a differentiated globular pro-embryo enclosed by a mature seed coat (Fig. 2k–l).

Functional and topological architecture of the co-expression network during the flower-to-fruit transition

A global gene co-expression network was constructed from 5,414 variance-filtered genes and organized into nine functional modules with high intramodular connectivity (Fig. 3a and S7). To characterize their functional organization during the FFT in *V. planifolia*, GO and KEGG pathway enrichment analyses were performed.

The green module was enriched in metabolic regulation, anatomical development, and gene expression control (Fig. 3c), whereas the dark grey module was associated with reproductive development and multicellular structure formation (Fig. 3d). The brown module showed enrichment in RNA-related processes and transcriptional regulation (Fig. 3e), and the turquoise module was linked to general metabolic and cellular functions. The dark orange module was enriched in nucleic acid metabolism, while the dark green module was associated with cellular regulation, multicellular development, and negative regulation of metabolism. The red module showed enrichment in developmental and epigenetic processes, including chromatin organization and remodeling. Although the pink module did not show significant GO enrichment, its gene composition suggests a potential role in chromatin remodeling during gametogenesis. Finally, the green-yellow module was associated with negative regulation of cellular processes, including protein localization to the vacuole and exocytosis-related functions (Supplementary Fig. S15).

Consistently, KEGG analysis identified hormone signal transduction as the most represented pathway across modules (Supplementary Figs. S8–S10). Based on this functional framework, highly connected genes were identified as hub nodes, representing the core regulatory architecture of each module (Supplementary Figs. S11–S14).

Integration of multiple regulatory dimensions in the modular organization of the transcriptional network during the flower-to-fruit transition

To interpret the topology and putative functions of the transcriptional network during the FFT, nine gene labels were generated and grouped into functional and structural categories, capturing key regulatory dimensions of the system. Functional labels included transcription factors (TF; 1,817 genes) and epigenetic regulators (EpiReg; 945), followed by conserved orthologs (C-Orth; 86) and stage-associated signatures (Pre-pol, Pol, Post-pol and Fer). Structural labels comprised differentially expressed genes (DEG; 1,091) and module hub genes (Hub; 491) (Fig. 4a).

Label intersections revealed recurrent combinations, with DEG + Hub being the most abundant, followed by Hub + TF and C-Orth + DEG, whereas higher-order combinations (DEG + Hub + TF + C-Orth) were less frequent (Fig. 4b; Table S2). These patterns reflect the convergence of multiple regulatory layers within the network. To contextualize these intersections, labels were mapped onto co-expression modules, which were prioritized based on connectivity, size, enrichment, and biological relevance (Fig. 4c; Supplementary Figs. S16–S17).

At the modular level, the green module exhibited a dense regulatory core characterized by intersections among DEG, TF, EpiReg, and C-Orth, consistent with the integration of metabolic and developmental processes. Similarly, the dark grey module was associated with reproductive regulation, with a high prevalence of Hub + TF and Hub + EpiReg intersections. The pink module displayed a compact core of transcriptional and epigenetic regulators, suggesting a specialized role in epigenetic regulation during megagametogenesis (Fig. 4c–e).

Candidate gene prioritization based on functional and structural labels during the flower-to-fruit transition in *Vanilla planifolia*

To prioritize candidate regulators of the FFT in *V. planifolia*, genes showing co-occurrence of at least one functional and one structural label were selected, yielding 88 candidates (Fig. 5; Supplementary Table S2). These were grouped into three categories:

(1) Type I, conserved transcriptional regulatory core: genes that are both conserved and central within the network (C-Orth + Hub; 4 genes).

(2) Type II, dynamic regulators: central transcription factors (Hub + TF; 22 genes), central epigenetic regulators (Hub + EpiReg; 10 genes), conserved genes with differential expression (C-Orth + DEG; 21 genes; Table S5), and regulators with dynamic expression profiles (TF + DEG; 9 genes; EpiReg + DEG; 1 gene).

(3) *Type III, stage-associated regulators:* genes with stage-associated differential expression during Pollination (DEG + Pol; 1 gene), Post-pollination (DEG + Post-pol; 6 genes), and Fertilization (DEG + Fer; 12 genes), and central genes associated with Fertilization (Hub + Fer; 2 genes). No genes with co-occurring labels were identified at the Pre-pollination stage. (Fig. 5; Supplementary Table S2).

Discussion

The flower-to-fruit transition as an integrated regulatory system

Complex biological systems are composed of dynamically interacting components whose organization and behavior emerge from these interactions and are structured into functional modules (Kitano 2002; Barabási et al. 2004). Within this framework, the FFT can be viewed as a complex biological system, in which coordinated interactions among multiple components give rise to developmental transitions as emergent properties (O'Neill 1997; Levine et al. 2005; Jaeger et al. 2014; Pajoro et al. 2014). From this perspective, in this work co-expression network analysis enabled the interpretation of the FFT as an integrated regulatory system, characterized by a modular and hierarchical organization defined by modules and genes with varying degrees of connectivity and centrality (Fig. 3a, b; Supplementary Figs. S11–S14). Consistent with this organization, here nine modules were identified and associated with key processes underlying the FFT and the PPS, including metabolic regulation and anatomical development,

reproductive regulation, epigenetic processes during megagametogenesis, multicellular structure formation, and nucleic acid metabolism (Fig. 3; Supplementary Fig. S15). Together, our results support the view that multiple biological processes are coordinated within an integrated regulatory framework during the FFT.

Co-expression networks as a structural and functional framework for candidate regulator prioritization

WGCNA-based analysis enables the description of regulatory architecture from a complex systems perspective (Langfelder et al. 2008), but does not inherently assign biological meaning to identified modules or genes (Langfelder et al. 2008; Yang et al. 2023). To address this limitation, structural and functional dimensions were incorporated into module-specific networks through nine flower-to-fruit transition labels (Fig. 4a), enabling the integration of network organization with biological function. This approach revealed diverse combinations of label intersections (Fig. 4b) and supported the definition of a classification framework that integrates structural and functional labels to assign putative roles to genes within the network (Fig. 5). Within this framework, three categories of candidate regulators were identified:

Type I corresponds to a conserved transcriptional regulatory core, comprising evolutionarily conserved genes that occupy central positions within the network as hub genes, consistent with preferential attachment processes (Fitch 1970; Koonin 2005; Prud'homme et al. 2007; Romero-Campero et al. 2013) (Fig. 5).

Type II includes dynamic regulators, encompassing: (i) hub genes and transcription factors, which may act as master regulators controlling multiple targets (Heyndrickx et al. 2014); (ii) hub genes and epigenetic regulators, associated with chromatin remodeling and transcriptional plasticity (Grant-Downton et al. 2005; Lin et al. 2013); (iii) conserved and differentially expressed genes (C-Orth + DEG), potentially linked to ancestral regulatory mechanisms (Palande et al. 2023); (iv) TF combined with DEG, which may fine-tune transcriptional changes during development (Riechmann et al. 2000; Theissen 2007; Karlova et al. 2014); and (v) EpiReg combined with DEG, potentially associated with epigenetic reprogramming processes underlying shifts in gene expression states (Hemenway et al. 2023; Ming et al. 2023) (Fig. 5).

Finally, Type III comprises stage-associated regulators identified based on stage-specific expression or their central roles within co-expression modules, consistent with temporally coordinated regulatory programs during the molecular phenology of the FFT (Kudoh 2016; Serin et al. 2016) (Fig. 5).

Candidate regulators within co-expression modules reflect the organization of the post-pollination syndrome

To characterize regulatory functions during the FFT in *V. planifolia*, candidate genes were examined in the context of co-expression modules.

The green module was associated with metabolic regulation and anatomical development (Fig. 3c; Supplementary Table S2), including genes related to hormone signaling and floral maturation (*VpGID1C*, *VpGASA11*, *VpIAA27*, *VpPRR73*, *VpASIL2*) (Griffiths et al. 2006; Willmann et al. 2011; Bassa et al. 2012; Ford et al. 2016; Gao et al. 2021). It also included genes linked to seed and fruit development (*VpRSCA*, *VpADH2*, *VpNAC074*), consistent with the reactivation of floral and ovule developmental programs during the PPS (O'Neill 1997; Ohnuma et al. 2004; Jin et al. 2016; Hernández-Miranda et al. 2020; Peng et al. 2023; Pérez-Posadas et al. 2024).

The darkgrey module included genes associated with ovary development and defense responses (Fig. 3d; Supplementary Table S2) (*VpAAE3*, *VpAIP1*, *VpPR1*, *VpWSCI*) (Di Gennaro et al. 2005; Li et al. 2011; Jin et al. 2021; Han et al. 2023). In species exhibiting post-pollination syndrome, prolonged ovary development increases exposure to environmental factors, requiring coordinated defense responses. In this context, this module suggests a transcriptional balance between reproductive growth and defense (Figueroa-Macías et al. 2021; Hernández-Miranda et al. 2025).

The brown module was enriched in transcriptional regulators (Fig. 3e; Supplementary Table S2) (*VpHUA1*, *VpSPL18*, *VpCYP78A5*, *VpNAC083*) involved in floral identity, organ architecture, and stress responses, consistent with a central regulatory role during the FFT (Chen et al. 1999; Lu et al. 2002; Eriksson et al. 2010; Suyal et al. 2014; Serin et al. 2016; Bai et al. 2021).

The turquoise module grouped genes associated with cellular metabolism and structural remodeling (Supplementary Fig. S15a; Supplementary Table S2) (*VpBHLH25*, *VpHHO3*, *VpFAS2*, *VpNAP2*), consistent with metabolic reprogramming and cell wall remodeling during early fruit development in angiosperms (Osorio et al. 2013; Hernández-Miranda et al. 2020).

The darkorange module included *BASIC HELIX–LOOP–HELIX 48 (VpBHLH48)*, *HOMEOBOX PROTEIN 6 (VpHOX6)*, and *TEOSINTE BRANCHED1/CYCLOIDEA/PCF 4 (VpTCP4)*, linking transcriptional and RNA-related (Supplementary Fig. S15b; Supplementary Table S2) processes with gynoecium development and environmental responses, consistent with high transcriptional demand during the FFT (Meijer et al. 2000; Wei et al. 2015; Hernández-Miranda et al. 2020; Yang et al. 2021; Li et al. 2025).

The darkgreen module integrated hormonal and developmental regulators (Supplementary Fig. S15c; Supplementary Table S2) (*VpCRL5, VpMYB105, VpCDC20.1, VpELP2*, and *VpMADS16*) and is proposed to coordinate hormone-dependent cell division and expansion following pollination (Kevei et al. 2011; Kitomi et al. 2011; Lee et al. 2003; O'Neill 1997; Quinet et al. 2019; Wu et al. 2021; Zhou et al. 2009).

The red module was represented by *AUXIN RESPONSE FACTOR 5 (VpARF5)*, a transcription factor known to recruit witch/sucrose non-fermentable (SWI/SNF) chromatin remodeling complexes, suggesting a role for epigenetic regulation in transcriptional reprogramming during the FFT (Rudolf et al. 2024) (Supplementary Fig. S15d; Supplementary Table S2).

The pink module included *CHROMATIN REMODELING 12 (VpCHR12)* and *MALE STERILITY PROTEIN 1 (VpMSP1)*, genes associated with chromatin remodeling (Supplementary Fig. S15e; Supplementary Table S2) and ovule cell fate determination. In *V. planifolia*, where ovule development is reactivated after pollination and remains environmentally responsive, this module is consistent with coordinated regulation of ovule maturation under post-pollination conditions (O'Neill 1997; Nonomura et al. 2003; Mlynárová et al. 2007; Hernández-Miranda et al. 2020).

Finally, the green-yellow module included *RADICAL-INDUCED CELL DEATH PROTEIN 16 (VpRAD16)*, associated with DNA repair and genome stability, processes essential for embryonic viability and consistent with a protective role during early development under environmental stress (Alrayes et al. 2023; Asik et al. 2026) (Supplementary Fig. S15f; Supplementary Table S2).

Putative functions of candidate genes in the anatomical context of the post-pollination syndrome

Based on candidate gene analysis, anatomical characterization, and functional evidence from homologous genes in other plant species, putative roles were assigned to candidate genes within the context of the FFT and the PPS in *V. planifolia* (Figs. 2–6; Supplementary Table S2).

Stage 1: Pre-pollination

The floral bud is formed but lacks fully developed ovules and exhibits placental projections (Fig. 2). *ARABIDOPSIS 6B-INTERACTING PROTEIN-LIKE 2 (VpASIL2)* is likely involved in maintaining ovule immaturity (Willmann et al. 2011), whereas *HUA ENHANCER 1 (VpHUA1), MYB TRANSCRIPTION FACTOR 105 (VpMYB105), MADS-BOX TRANSCRIPTION FACTOR 16 (VpMADS16)* and *ABSCISIC ACID-INSENSITIVE PROTEIN 1 (VpAIP1)* are associated with floral identity and organ differentiation (Chen et al. 1999; Lee et al. 2003; Li et al. 2011; Wu et al. 2021). These processes are modulated by environmental response genes (*VpPRR73*, *VpPIL13*, *VpMYBS3*, *VpHHO3*) linked to light, temperature, and nitrogen signaling (Lu et al. 2002; Nakamura et al. 2007; Ford et al. 2016; Safi et al. 2018) (Fig. 6).

Stage 2: Pollination

During anthesis, environmental synchronization is associated with *PHYTOCHROME-INTERACTING FACTOR-LIKE 13 (VpPIL13), FAR-RED ELONGATED HYPOCOTYL 3-LIKE 5 (VpFRS5)*, and *VpBHLH48* (Ji et al. 2019; Yang et al. 2021; Kim et al. 2025). Pollination induces placental proliferation, differentiation of transmitting tissue, and pollen tube growth (Fig. 2), a process supported by *OIL BODY LIPASE 1 (VpOBL1)* (Müller et al. 2018). Ovule development is initiated concurrently, with hormonal reprogramming mediated by auxins and gibberellins (*VpGID1C*, *VpIAA27*, *VpARF5*, *VpGASA11*, *VpWRKY24*, *VpCRL5*) likely contributing to gynoecium reactivation through downstream regulators such as *SQUAMOSA PROMOTER-BINDING PROTEIN-LIKE 18 (VpSPL18), CELL DIVISION CYCLE 20.1 (VpCDC20.1), FATTY ACID SYNTHASE 2 (VpFAS2)*, and *VpTCP4* (Griffiths et al. 2006; Chen et al. 2008; Kitomi et al. 2011; Kevei et al. 2011; Bassa et al. 2012; Wei et al. 2015; Gao et al. 2021; Bai et al. 2021; Rudolf et al. 2024) (Fig. 6).

Stage 3: Post-pollination

The functional megaspore develops into the embryo sac, accompanied by nucellar reduction and integument differentiation (Fig. 2). *INDOLE-3-ACETIC ACID-INDUCIBLE PROTEIN 6* (*VpIAA6*), together with *BURP DOMAIN-CONTAINING PROTEIN 3 (VpBURP3), HEAVY METAL-ASSOCIATED ISOPRENYLATED PLANT PROTEIN 36 (VpHIPP36)*, and *VERY-LONG-CHAIN ALDEHYDE DECARBONYLASE GL1-4 (VpGL1-4)*, is associated with the integration of hormonal signaling and cell wall remodeling (Koshiba et al. 1995; Islam et al. 2009; Leonte 2021; Kavas et al. 2021). During this prolonged phase, stress responses to heat, light, water deficit, and defense are activated (*VpHSFA2D*, *VpHSFB2B*, *VpHSFB4*, *VpAPRR3*, *VpRAD16*, *VpHOX6*, *VpPER55*, *VpELI3*, *VpCER2*) (Kiedrowski et al. 1992; Meijer et al. 2000; Matsushika et al. 2000; Ikeda et al. 2011; Begum et al. 2013; Pascal et al. 2013; Zhang et al. 2018; Mase et al. 2021; Alrayes et al. 2023; Asik et al. 2026), coordinated with hormonal regulation (*VpBGLU9*, *VpWRKY24*, *VpWRKY70*) (Atamian et al. 2012; Li et al. 2024; Yang et al. 2024). Additionally, *ELONGATOR COMPLEX PROTEIN 2* (*VpELP2*) and *YIN YANG 1 TRANSCRIPTION FACTOR* **(***VpYY1)* are associated with ABA-dependent pathways (Zhou et al. 2009; Li et al. 2016), while *VpCHR12* and *VpMSP1* may contribute to transient developmental arrest under stress conditions (Nonomura et al. 2003; Hernández-Miranda et al. 2020) (Fig. 6).

Stage 4: Fertilization

The embryo sacs develop into embryos, accompanied by nucellar degeneration, suspensor formation, and seed coat differentiation (Fig. 2). These processes involve *NAC DOMAIN-CONTAINING PROTEIN 74 (VpNAC074), PHYTOCHROME INTERACTING FACTOR-LIKE 15 (VpPIL15)*, and *BASIC LEUCINE ZIPPER 44 (VpBZIP44)*, and *INDOLE-3-ACETIC ACID-INDUCIBLE PROTEIN 27 (VpIAA27)*, which are associated with hormonal regulation and seed size control (Bassa et al. 2012; Iglesias-Fernández et al. 2013; Ji et al. 2019; Peng et al. 2023). Fruit maturation is supported by genes involved in cell wall modification (*VpBURP3*, *Vp4CL1*, *VpMIZ1*, *VpCYP78A5*) (Wu et al. 1997; Eriksson et al. 2010; Li et al. 2015; Kavas et al. 2021), as well as genes associated with fruit development (*VpADH2*, *VpNAP2*). Given the prolonged fruit development in *V. planifolia*, defense-related genes (*VpRSCA*, *VpAAE3*, *VpWSCI*, *VpPR1*) remain active (Ohnuma et al. 2004; Di Gennaro et al. 2005; Jin et al. 2016; Ma et al. 2018; Han et al. 2023) (Fig. 6).

Scope and limitations

This study provides a working framework for investigating the PPS, particularly in orchids such as *V. planifolia*, for which genomic resources remain limited. By integrating structural and functional labels within a systems-level transcriptomic framework, our approach combines network topology with functional information from model and non-model angiosperms to characterize co-expression modules and prioritize candidate genes (Stuart et al. 2003; Zhang et al. 2005).

However, the resulting associations are inferential and should not be interpreted as evidence of causal regulatory relationships (Stuart et al. 2003; Langfelder et al. 2008). Functional assignments rely partly on orthology and evidence from other species and may therefore not fully reflect gene functions in *V.*

planifolia (Rhee et al. 2008; Radivojac et al. 2013). Moreover, gene expression and network organization may vary across environmental, temporal, and genotypic contexts (Fornara et al. 2010; Kazan et al. 2016). Thus, the 88 prioritized genes should be considered candidates for future experimental validation rather than functionally confirmed regulators.

Conclusion

A systems-level transcriptomic approach enabled the inference of a co-expression network associated with the PPS, revealing nine functional modules linked to reproductive development, metabolic regulation, gene expression, nucleic acid metabolism, and epigenetic regulation, with hormone signaling emerging as a central component. These findings support the interpretation of the FFT as an integrated regulatory system. Within this framework, 88 candidate genes were prioritized through the intersection of structural and functional network dimensions, capturing major aspects of FFT transcriptional dynamics, including ovule and ovary repression and reactivation, hormonal modulation, fruit development, and defense and environmental responses. Integration of the co-expression network with anatomical context further placed these molecular processes within developmental progression, providing a systems-level framework for understanding the post-pollination syndrome. Overall, this study establishes a reproducible and generalizable strategy for identifying and prioritizing candidate regulatory genes in non-model plants undergoing complex reproductive transitions.

Declarations

Acknowledgements

This manuscript is part of OAHM dissertation for the Ph.D. in Sciences in the Posgrado en Ciencias Biológicas (PCB), UNAM. OAHM also thanks the Secretaría de Ciencia, Humanidades, Tecnología e Innovación (SECIHITI) for the doctoral fellowship supporting this work (Fellowship number, 33716). We are grateful to the vanilla producers of the Totonacapan region, particularly Mr. Miguel Acosta, for their valuable collaboration and contribution to this study.

Supplementary Information

The online version contains supplementary material available at:
https://doi.org/10.5281/zenodo.20018940

Author contributions

OAHM, VMSR, JEC, UR, and ESZ conceived and designed the study. OAHM and VMSR performed the transcriptomic analyses, co-expression network reconstruction, functional enrichment analyses, and candidate gene prioritization. ASBA, JAVG, MCGR, and ESZ conducted and interpreted the anatomical analyses. OAHM, VMSR, ESZ, JEC, ASBA, JAVG, and UR integrated and interpreted the molecular and anatomical data. OAHM, ASBA, JAVG, VMSR, UR, JEC, ESZ, and MCGR curated the data. OAHM, VMSR,

ESZ, ASBA, and JAVG wrote the original draft of the manuscript. VMSR, UR, JEC, and ESZ supervised the study. All authors reviewed, edited, and approved the final manuscript.

Funding

This work was financially supported by El Fondo Sectorial de Investigación para la Educación (SEP-CONACYT), Basic Scientific Research 2015, Project 255952 awarded to VMSR.

Data availability

All raw sequencing data are available in the NCBI BioProject under accession number PRJNA808623. The assembled and annotated transcriptome is available at Zenodo: https://doi.org/10.5281/zenodo.18765805. The integrated dataset used for comparative analyses is available at Zenodo: https://doi.org/10.5281/zenodo.18795437. Supplementary datasets, including processed data and intermediate results, are available at Zenodo: https://doi.org/10.5281/zenodo.20018940 and https://doi.org/10.5281/zenodo.20336749.

Conflict of interest The authors declare that they have no conflict of interest.

References

1. Aerts S, Lambrechts D, Maity S, Van Loo P, Coessens B, De Smet F et al (2006) Gene prioritization through genomic data fusion. Nat Biotechnol 24(5):537–544.
2. Alrayes L, Stout J, Schroeder D (2023) Arabidopsis RAD16 homologues are involved in UV tolerance and growth. Genes 14(8):1552.
3. Asik E, Kashif SZ, Oztas O (2026) Plant tolerance mechanisms to DNA-damaging UV stress. J Exp Bot 77(1):27–50.
4. Atamian HS, Eulgem T, Kaloshian I (2012) SlWRKY70 is required for Mi-1-mediated resistance to aphids and nematodes in tomato. Planta 235(2):299–309.
5. Bai S, Hong J, Li L, Su S, Li Z, Wang W et al (2021) Dissection of the genetic basis of rice panicle architecture using a genome-wide association study. Rice 14(1):77.
6. Barabasi AL, Oltvai ZN (2004) Network biology: understanding the cell's functional organization. Nat Rev Genet 5(2):101–113.
7. Bassa C, Mila I, Bouzayen M, Audran-Delalande C (2012) Phenotypes associated with down-regulation of Sl-IAA27 support functional diversity among Aux/IAA family members in tomato. Plant Cell Physiol 53(9):1583–1595.
8. Begum T, Reuter R, Schöffl F (2013) Overexpression of AtHsfB4 induces specific effects on root development of Arabidopsis. Mech Dev 130(1):54–60.
9. Bolser D, Staines DM, Pritchard E, Kersey P (2016) Ensembl plants: integrating tools for visualizing, mining, and analyzing plant genomics data. In Plant bioinformatics: Methods and protocols (pp. 115–140). New York, NY: Springer New York.

10. Busser BW, Bulyk ML, Michelson AM (2008) Toward a systems-level understanding of developmental regulatory networks. Curr Opin Genet Dev 18(6):521–529.
11. Chen X, Meyerowitz EM (1999) HUA1 and HUA2 are two members of the floral homeotic AGAMOUS pathway. Mol Cell 3(3):349–360.
12. Chen Z, Tan JLH, Ingouff M, Sundaresan V, Berger F (2008) Chromatin assembly factor 1 regulates the cell cycle but not cell fate during male gametogenesis in Arabidopsis thaliana. Development 135(1):65–73. https://doi.org/10.1242/dev.010108
13. Chevalier É, Loubert-Hudon A, Zimmerman EL, Matton DP (2011) Cell–cell communication and signalling pathways within the ovule: From its inception to fertilization. New Phytol 192(1):13–28. https://doi.org/10.1111/j.1469–8137.2011.03836.x
14. Cooper L, Elser J, Laporte MA, Arnaud E, Jaiswal P (2024) Planteome 2024 update: reference ontologies and knowledgebase for plant biology. Nucleic Acids Res 52(D1):D1548-D1555.
15. Di Gennaro S, Ficca AG, Panichi D, Poerio E (2005) cDNA cloning and heterologous expression of a wheat proteinase inhibitor of subtilisin and chymotrypsin (WSCI) that interferes with digestive enzymes of insect pests. Biol Chem 386(4):383–389.
16. Emms DM, Kelly S (2019) OrthoFinder: phylogenetic orthology inference for comparative genomics. Genome Biol 20(1):238.
17. Endress PK (2011) Angiosperm ovules: diversity, development, evolution. Ann Bot 107(9):1465–1489.
18. Eriksson S, Stransfeld L, Adamski NM, Breuninger H, Lenhard M (2010) KLUH/CYP78A5-dependent growth signaling coordinates floral organ growth in Arabidopsis. Curr Biol 20(6):527–532.
19. Feng X, Liu S, Cheng H, Zuo D, Zhang Y, Wang Q et al (2021) Weighted gene co-expression network analysis reveals hub genes contributing to fuzz development in Gossypium arboreum. Genes 12(5):753.
20. Figueroa-Macías JP, García YC, Núñez M, Díaz K, Olea AF, Espinoza L (2021) Plant growth-defense trade-offs: molecular processes leading to physiological changes. Int J Mol Sci 22(2):693.
21. Fitch WM (1970) Distinguishing homologous from analogous proteins. Syst Zool 19(2):99–113.
22. Ford B, Deng W, Clausen J, Oliver S, Boden S, Hemming M, Trevaskis B (2016) Barley (Hordeum vulgare) circadian clock genes can respond rapidly to temperature in an EARLY FLOWERING 3-dependent manner. J Exp Bot 67(18):5517–5528.
23. Fornara F, de Montaigu A, Coupland G (2010) SnapShot: control of flowering in Arabidopsis. Cell 141(3):550–550.
24. Gao X, Guo F, Chen Y, Bai G, Liu Y, Jin J, Wang Q (2021) Full-length transcriptome analysis provides new insights into the early bolting occurrence in medicinal Angelica sinensis. Sci Rep 11(1):13000.
25. Grant-Downton R, Dickinson HG (2005) Epigenetics and its implications for plant biology. 1. The epigenetic network in plants. Ann Bot 96(7):1143–1164.

26. Griffiths J, Murase K, Rieu I, Zentella R, Zhang ZL, Powers SJ et al (2006) Genetic characterization and functional analysis of the GID1 gibberellin receptors in Arabidopsis. Plant Cell 18(12):3399–3414.
27. Han Z, Xiong D, Schneiter R, Tian C (2023) The function of plant PR1 and other members of the CAP protein superfamily in plant–pathogen interactions. Mol Plant Pathol 24(6):651–668.
28. Hemenway EA, Gehring M (2023) Epigenetic regulation during plant development and the capacity for epigenetic memory. Annu Rev Plant Biol 74(1):87–109.
29. Hernández-Miranda OA, Reyes-Mateos DA, Campos JE, Sandoval-Zapotitla E, Herrera-Cabrera BE, Salazar-Rojas VM (2020) Expresión diferencial del complejo ARF8-IAA25-like-TIR1 durante el síndrome postpolinización en dos genotipos de vainilla. Revista Fitotecnia Mexicana 43(4A):575–582.
30. Hernández-Miranda OA, Campos JE, Sandoval-Zapotitla E, Rosas U, Ortiz-Melo MT, Salazar-Rojas VM (2025) Transcriptomic analysis reveals molecular phenological changes during the flower-to-fruit transition in Vanilla planifolia Andrews (Orchidaceae). BMC Plant Biol 25(1):1–18.
31. Heyndrickx KS, de Velde JV, Wang C, Weigel D, Vandepoele K (2014) A functional and evolutionary perspective on transcription factor binding in Arabidopsis thaliana. Plant Cell 26(10):3894–3910.
32. Iglesias-Fernández R, Barrero-Sicilia C, Carrillo-Barral N, Oñate-Sánchez L, Carbonero P (2013) Arabidopsis thaliana bZIP 44: a transcription factor affecting seed germination and expression of the mannanase-encoding gene AtMAN7. Plant J 74(5):767–780.
33. Ikeda M, Mitsuda N, Ohme-Takagi M (2011) Arabidopsis HsfB1 and HsfB2b act as repressors of the expression of heat-inducible Hsfs but positively regulate the acquired thermotolerance. Plant Physiol 157(3):1243–1254.
34. Islam MA, Du H, Ning J, Ye H, Xiong L (2009) Characterization of Glossy1-homologous genes in rice involved in leaf wax accumulation and drought resistance. Plant Mol Biol 70(4):443–456.
35. Jaeger J, Monk N (2014) Bioattractors: dynamical systems theory and the evolution of regulatory processes. J Physiol 592(11):2267–2281.
36. Ji X, Du Y, Li F, Sun H, Zhang J, Li J et al (2019) The basic helix-loop-helix transcription factor, Os PIL 15, regulates grain size via directly targeting a purine permease gene Os PUP 7 in rice. Plant Biotechnol J 17(8):1527–1537.
37. Jin J, Tian F, Yang D-C, Meng Y-Q, Kong L, Luo J, Gao G (2017) PlantTFDB 4.0: Toward a central hub for transcription factors and regulatory interactions in plants. Nucleic Acids Res 45(D1):D1040–D1045. https://doi.org/10.1093/nar/gkw982
38. Jin Y, Zhang C, Liu W, Tang Y, Qi H, Chen H, Cao S (2016) The alcohol dehydrogenase gene family in melon (Cucumis melo L.): bioinformatic analysis and expression patterns. Front Plant Sci 7:670.
39. Jin JF, He QY, Li PF, Lou HQ, Chen WW, Yang JL (2021) Genome-wide identification and gene expression analysis of acyl-activating enzymes superfamily in tomato (Solanum lycopersicum) under aluminum stress. Front Plant Sci 12:754147.

40. Kanehisa M, Goto S (2000) KEGG: kyoto encyclopedia of genes and genomes. Nucleic Acids Res 28(1):27–30.
41. Karlova R, Chapman N, David K, Angenent GC, Seymour GB, De Maagd RA (2014) Transcriptional control of fleshy fruit development and ripening. J Exp Bot 65(16):4527–4541.
42. Kavas M, Yıldırım K, Seçgin Z, Abdulla MF, Gökdemir G (2021) Genome-wide identification of the BURP domain-containing genes in Phaseolus vulgaris. Physiol Mol Biol Plants 27(9):1885–1902.
43. Kazan K, Lyons R (2016) The link between flowering time and stress tolerance. J Exp Bot 67(1):47–60.
44. Kevei Z, Baloban M, Da Ines O, Tiricz H, Kroll A, Regulski K et al (2011) Conserved CDC20 cell cycle functions are carried out by two of the five isoforms in Arabidopsis thaliana. PLoS One 6(6):e20618.
45. Kiedrowski S, Kawalleck P, Hahlbrock K, Somssich IE, Dangl JL (1992) Rapid activation of a novel plant defense gene is strictly dependent on the Arabidopsis RPM1 disease resistance locus. EMBO J 11(13):4677–4684.
46. Kim K, Choi G (2025) FAR1-RELATED SEQUENCE 5 prevents photobleaching under short days by balancing chlorophyll biosynthetic gene expression. Plant Physiol, 199(2), kiaf475.
47. Kitano H (2002) Systems biology: a brief overview. science 295(5560):1662–1664.
48. Kitomi Y, Ito H, Hobo T, Aya K, Kitano H, Inukai Y (2011) The auxin responsive AP2/ERF transcription factor CROWN ROOTLESS5 is involved in crown root initiation in rice through the induction of OsRR1, a type-A response regulator of cytokinin signaling. Plant J 67(3):472–484.
49. Koonin EV (2005) Orthologs, paralogs, and evolutionary genomics. Annu Rev Genet 39(1):309–338.
50. Koshiba T, Ballas N, Wong LM, Theologis A (1995) Transcriptional Regulation ofPS-IAA4/5andPS-IAA6Early Gene Expression by Indoleacetic Acid and Protein Synthesis Inhibitors in Pea (Pisum sativum). J Mol Biol 253(3):396–413.
51. Kudoh H (2016) Molecular phenology in plants: in natura systems biology for the comprehensive understanding of seasonal responses under natural environments. New Phytol 210(2):399–412.
52. Langfelder P, Horvath S (2008) WGCNA: an R package for weighted correlation network analysis. BMC Bioinformatics 9(1):559.
53. Lee S, Jeon JS, An K, Moon YH, Lee S, Chung YY, An G (2003) Alteration of floral organ identity in rice through ectopic expression of OsMADS16. Planta 217(6):904–911.
54. Leonte G (2021) Characterization of cluster-III HIPP proteins targeted to plasmodesmata in Arabidopsis thaliana (Doctoral dissertation).
55. Levine M, Davidson EH (2005) Gene regulatory networks for development. Proc Natl Acad Sci U S A 102:4936–4942. https://doi.org/10.1073/pnas.0408031102
56. Lex A, Gehlenborg N, Strobelt H, Vuillemot R, Pfister H (2014) UpSet: visualization of intersecting sets. IEEE Trans Vis Comput Graph 20(12):1983–1992.
57. Li X, Gao X, Wei Y, Deng L, Ouyang Y, Chen G et al (2011) Rice APOPTOSIS INHIBITOR5 coupled with two DEAD-box adenosine 5'-triphosphate-dependent RNA helicases regulates tapetum

degeneration. Plant Cell 23(4):1416–1434.
58. Li T, Huang J, Wang G, Li H, Lü P (2025) Regulatory roles of RNA modifications in plant development and fruit ripening. Abiotech 6(3):472–488.
59. Li GZ, Liu J, Wang YY, Han AQ, Liu HT, Guo TC et al (2024) TaWRKY24–1D, interacts with TaERFL1a, regulates DHAR-mediated ASA-GSH biosynthesis to enhance drought tolerance in wheat. Plant Growth Regul 104(2):713–725.
60. Li T, Wu XY, Li H, Song JH, Liu JY (2016) A dual-function transcription factor, AtYY1, is a novel negative regulator of the Arabidopsis ABA response network. Mol Plant 9(5):650–661.
61. Li Y, Kim JI, Pysh L, Chapple C (2015) Four isoforms of Arabidopsis 4-coumarate: CoA ligase have overlapping yet distinct roles in phenylpropanoid metabolism. Plant Physiol 169(4):2409–2421.
62. Lin M, Chen Q, Yan S (2013) Network in network. arXiv preprint arXiv:1312.4400.
63. Liu Y, Gu HY, Zhu J, Niu YM, Zhang C, Guo GL (2019) Identification of hub genes and key pathways associated with bipolar disorder based on weighted gene co-expression network analysis. Front Physiol 10:1081.
64. Lord EM, Russell SD (2002) The mechanisms of pollination and fertilization in plants. Annu Rev Cell Dev Biol 18(1):81–105.
65. Lu CA, Ho THD, Ho SL, Yu SM (2002) Three novel MYB proteins with one DNA binding repeat mediate sugar and hormone regulation of α-amylase gene expression. Plant Cell 14(8):1963–1980.
66. Ma X, Zhang Y, Turečková V, Xue GP, Fernie AR, Mueller-Roeber B, Balazadeh S (2018) The NAC transcription factor SlNAP2 regulates leaf senescence and fruit yield in tomato. Plant Physiol 177(3):1286–1302.
67. Mase K, Tsukagoshi H (2021) Reactive oxygen species link gene regulatory networks during Arabidopsis root development. Front Plant Sci 12:660274.
68. Matsushika A, Makino S, Kojima M, Mizuno T (2000) Circadian waves of expression of the APRR1/TOC1 family of pseudo-response regulators in Arabidopsis thaliana: insight into the plant circadian clock. Plant Cell Physiol 41(9):1002–1012.
69. Meijer AH, De Kam RJ, d'Erfurth I, Shen W, Hoge JHC (2000) HD-Zip proteins of families I and II from rice: interactions and functional properties. Mol Gen Genet 263(1):12–21.
70. Ming Y, Jiang L, Ji D (2023) Epigenetic regulation in tomato fruit ripening. Front Plant Sci 14:1269090.
71. Mlynárová L, Nap JP, Bisseling T (2007) The SWI/SNF chromatin-remodeling gene AtCHR12 mediates temporary growth arrest in Arabidopsis thaliana upon perceiving environmental stress. Plant J 51(5):874–885.
72. Müller AO, Ischebeck T (2018) Characterization of the enzymatic activity and physiological function of the lipid droplet-associated triacylglycerol lipase At OBL 1. New Phytol 217(3):1062–1076.
73. Nakamura Y, Kato T, Yamashino T, Murakami M, Mizuno T (2007) Characterization of a set of phytochrome-interacting factor-like bHLH proteins in Oryza sativa. Biosci Biotechnol Biochem

71(5):1183–1191.

74. Nonomura KI, Miyoshi K, Eiguchi M, Suzuki T, Miyao A, Hirochika H, Kurata N (2003) The MSP1 gene is necessary to restrict the number of cells entering into male and female sporogenesis and to initiate anther wall formation in rice. Plant Cell 15(8):1728–1739.
75. Ohnuma T, Taira T, Yamagami T, Aso Y, Ishiguro M (2004) Molecular cloning, functional expression, and mutagenesis of cDNA encoding class I chitinase from rye (Secale cereale) seeds. Biosci Biotechnol Biochem 68(2):324–332.
76. O'Neill SD (1997) Pollination Regulation of Flower Development. Annu Rev Plant Physiol Plant Mol Biol 48(1):547–574.
77. Osorio S, Scossa F, Fernie AR (2013) Molecular regulation of fruit ripening. Front Plant Sci 4:198.
78. Pajoro A, Biewers S, Dougali E, Leal Valentim F, Mendes MA, Porri A, Coupland G, Van de Peer Y, van Dijk ADJ, Colombo L, Davies B, Angenent GC (2014) The (r)evolution of gene regulatory networks controlling Arabidopsis plant reproduction: a two-decade history. J Exp Bot 65:4731–4745. https://doi.org/10.1093/jxb/eru233
79. Palande S, Kaste JA, Roberts MD, Segura Abá K, Claucherty C, Dacon J et al (2023) Topological data analysis reveals a core gene expression backbone that defines form and function across flowering plants. PLoS Biol 21(12):e3002397.
80. Pascal S, Bernard A, Sorel M, Pervent M, Vile D, Haslam RP et al (2013) The A rabidopsis cer26 mutant, like the cer2 mutant, is specifically affected in the very long chain fatty acid elongation process. Plant J 73(5):733–746.
81. Pavlopoulos GA, Malliarakis D, Papanikolaou N, Theodosiou T, Enright AJ, Iliopoulos I (2015) Visualizing genome and systems biology: technologies, tools, implementation techniques and trends, past, present and future. GigaScience 4(1):s13742–015.
82. Peng B, Sun X, Tian X, Kong D, He L, Peng J et al (2023) OsNAC74 affects grain protein content and various biological traits by regulating OsAAP6 expression in rice. Mol Breed 43(12):87.
83. Pérez-Posadas M, Zavaleta-Mancera HA, Delgado-Alvarado A, Salazar-Rojas VM, Herrera-Cabrera BE (2024) Morphological identification and characterization of the formation of floral primordium in Vanilla planifolia (Orchidaceae). Agroproductividad 17(6):161–169.
84. Prud'homme B, Gompel N, Carroll SB (2007) Emerging principles of regulatory evolution. Proc Natl Acad Sci U S A 104(suppl_1):8605–8612.
85. Quinet M, Angosto T, Yuste-Lisbona FJ, Blanchard-Gros R, Bigot S, Martinez JP, Lutts S (2019) Tomato fruit development and metabolism. Front Plant Sci 10:1554.
86. Radivojac P, Clark WT, Oron TR, Schnoes AM, Wittkop T, Sokolov A et al (2013) A large-scale evaluation of computational protein function prediction. Nat Methods 10(3):221–227.
87. Raudvere U, Kolberg L, Kuzmin I, Arak T, Adler P, Peterson H, Vilo J (2019) g: Profiler: a web server for functional enrichment analysis and conversions of gene lists (2019 update). Nucleic Acids Res 47(W1):W191-W198.

88. Rhee SY, Wood V, Dolinski K, Draghici S (2008) Use and misuse of the gene ontology annotations. Nat Rev Genet 9(7):509–515. https://doi.org/10.1038/nrg2363
89. Riechmann JL, Ratcliffe OJ (2000) A genomic perspective on plant transcription factors. Curr Opin Plant Biol 3(5):423–434.
90. Romero-Campero FJ, Lucas-Reina E, Said FE, Romero JM, Valverde F (2013) A contribution to the study of plant development evolution based on gene co-expression networks. Front Plant Sci 4:291.
91. Ruan Y-L, Patrick JW, Bouzayen M, Osorio S, Fernie AR (2012) Molecular regulation of seed and fruit set. Trends Plant Sci 17(11):656–665. https://doi.org/10.1016/j.tplants.2012.06.005
92. Rudolf J, Tomovicova L, Panzarova K, Fajkus J, Hejatko J, Skalak J (2024) Epigenetics and plant hormone dynamics: a functional and methodological perspective. J Exp Bot 75(17):5267–5294.
93. Safi A, Medici A, Szponarski W, Marshall-Colon A, Ruffel S, Gaymard F et al (2018) HRS1/HHOs GARP transcription factors and reactive oxygen species are regulators of Arabidopsis nitrogen starvation response. BioRXiv, 164277.
94. Salazar-Rojas VM, Sandoval-Zapotitla E, Granados-Hernández CV, Cruz-Ruiz Y, Herrera-Cabrera BE, Campos-Contreras JE (2016) Descripcion estructural y funcional de caida prematura de frutos DE Vanilla planifolia Jacks. ex Andrew. Agroproductividad 9(S1):17–20.
95. Sandoval ZE, Rojas LA, Guzmán RC, Carmona JL, Ponce RM et al (2005) Cuadernos 38: técnicas aplicadas al estudio de la anatomía vegetal. Universidad Nacional Autónoma de México.
96. Serin EA, Nijveen H, Hilhorst HW, Ligterink W (2016) Learning from co-expression networks: possibilities and challenges. Front Plant Sci 7:444.
97. Shahan R, Zawora C, Wight H, Sittmann J, Wang W, Mount SM, Liu Z (2018) Consensus coexpression network analysis identifies key regulators of flower and fruit development in wild strawberry. Plant Physiol 178(1):202–216.
98. Stuart JM, Segal E, Koller D, Kim SK (2003) A gene-coexpression network for global discovery of conserved genetic modules. science 302(5643):249–255.
99. Suyal G, Rana VS, Mukherjee SK, Wajid S, Choudhury NR (2014) Arabidopsis thaliana NAC083 protein interacts with Mungbean yellow mosaic India virus (MYMIV) Rep protein. Virus Genes 48(3):486–493.
100. Theissen G, Melzer R (2007) Molecular mechanisms underlying origin and diversification of the angiosperm flower. Ann Bot 100(3):603–619.
101. Tornielli GB, Sandri M, Fasoli M, Amato A, Pezzotti M, Zuccolotto P, Zenoni S (2023) A molecular phenology scale of grape berry development. Hortic Res, 10(5), uhad048.
102. Van Bel M, Silvestri F, Weitz EM, Kreft L, Botzki A, Coppens F, Vandepoele K (2022) PLAZA 5.0: extending the scope and power of comparative and functional genomics in plants. Nucleic Acids Res 50(D1):D1468-D1474.
103. Wei B, Zhang J, Pang C, Yu H, Guo D, Jiang H et al (2015) The molecular mechanism of SPOROCYTELESS/NOZZLE in controlling Arabidopsis ovule development. Cell Res 25(1):121–134.

104. Willmann MR, Mehalick AJ, Packer RL, Jenik PD (2011) MicroRNAs regulate the timing of embryo maturation in Arabidopsis. Plant Physiol 155(4):1871–1884.
105. Wu W, Li J, Wang Q, Lv K, Du K, Zhang W et al (2021) Growth-regulating factor 5 (GRF5)-mediated gene regulatory network promotes leaf growth and expansion in poplar. New Phytol 230(2):612–628.
106. Wu L, Wu H, Sangiorgi F, Wu N, Bell JR, Lyons GE, Maxson R (1997) Miz1, a novel zinc finger transcription factor that interacts with Msx2 and enhances its affinity for DNA. Mech Dev 65(1–2):3–17.
107. Yang L, Yang L, Ding Y, Chen Y, Liu N, Zhou X et al (2023) Global transcriptome and co-expression network analyses revealed hub genes controlling seed size/weight and/or oil content in peanut. Plants 12(17):3144.
108. Yang C, Huang S, Zeng Y, Liu C, Ma Q, Pruneda-Paz J et al (2021) Two bHLH transcription factors, bHLH48 and bHLH60, associate with phytochrome interacting factor 7 to regulate hypocotyl elongation in Arabidopsis. Cell Rep, 35(5).
109. Yang H, Yao X, Wu W, He A, Ma C, Yang S, Ruan J (2024) Genome-wide identification and gene expression pattern analysis of the glycoside hydrolase family 1 in Fagopyrum tataricum. BMC Plant Biol 24(1):1183.
110. Zhang L, Chong Y, Yang X, Fan W, Cheng F, Li Y et al (2025) Comparative transcriptome reveals conserved gene expression in reproductive organs in Solanaceae. Int J Mol Sci 26(8):3568.
111. Zhang B, Horvath S (2005) A general framework for weighted gene co-expression network analysis. Stat Appl Genet Mol Biol 4(1):1128.
112. Zhang N, Yu H, Yu H, Cai Y, Huang L, Xu C et al (2018) A core regulatory pathway controlling rice tiller angle mediated by the LAZY1-dependent asymmetric distribution of auxin. Plant Cell 30(7):1461–1475.
113. Zhou X, Hua D, Chen Z, Zhou Z, Gong Z (2009) Elongator mediates ABA responses, oxidative stress resistance and anthocyanin biosynthesis in Arabidopsis. Plant J 60(1):79–90.

Figures

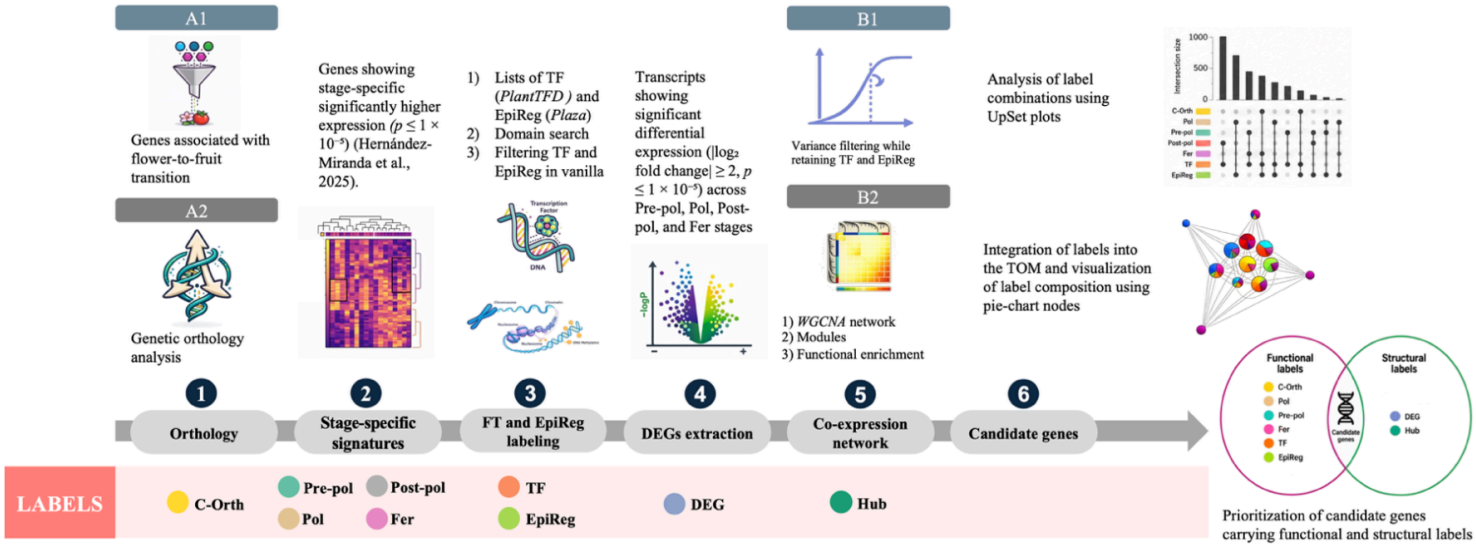


Figure 1

Workflow overview. The labels used represent different levels of functional and structural classification of the transcriptome. Structural labels (green circle) include differentially expressed genes (DEGs) and module hub genes (Hub). Functional labels (pink circle) include stage-associated genes (PrePol, Pol, PostPol, and Fer), conserved orthologs (C-Orth), transcription factors (TF), and epigenetic regulators (EpiReg). The developmental stages represented in the transcriptomes correspond to Pre-pollination (PrePol), Pollination (Pol), Post-pollination (PostPol), and Fertilization (Fer), collectively encompassing the flower-to-fruit transition (FFT). Workflow available at: https://doi.org/10.5281/zenodo.19993038

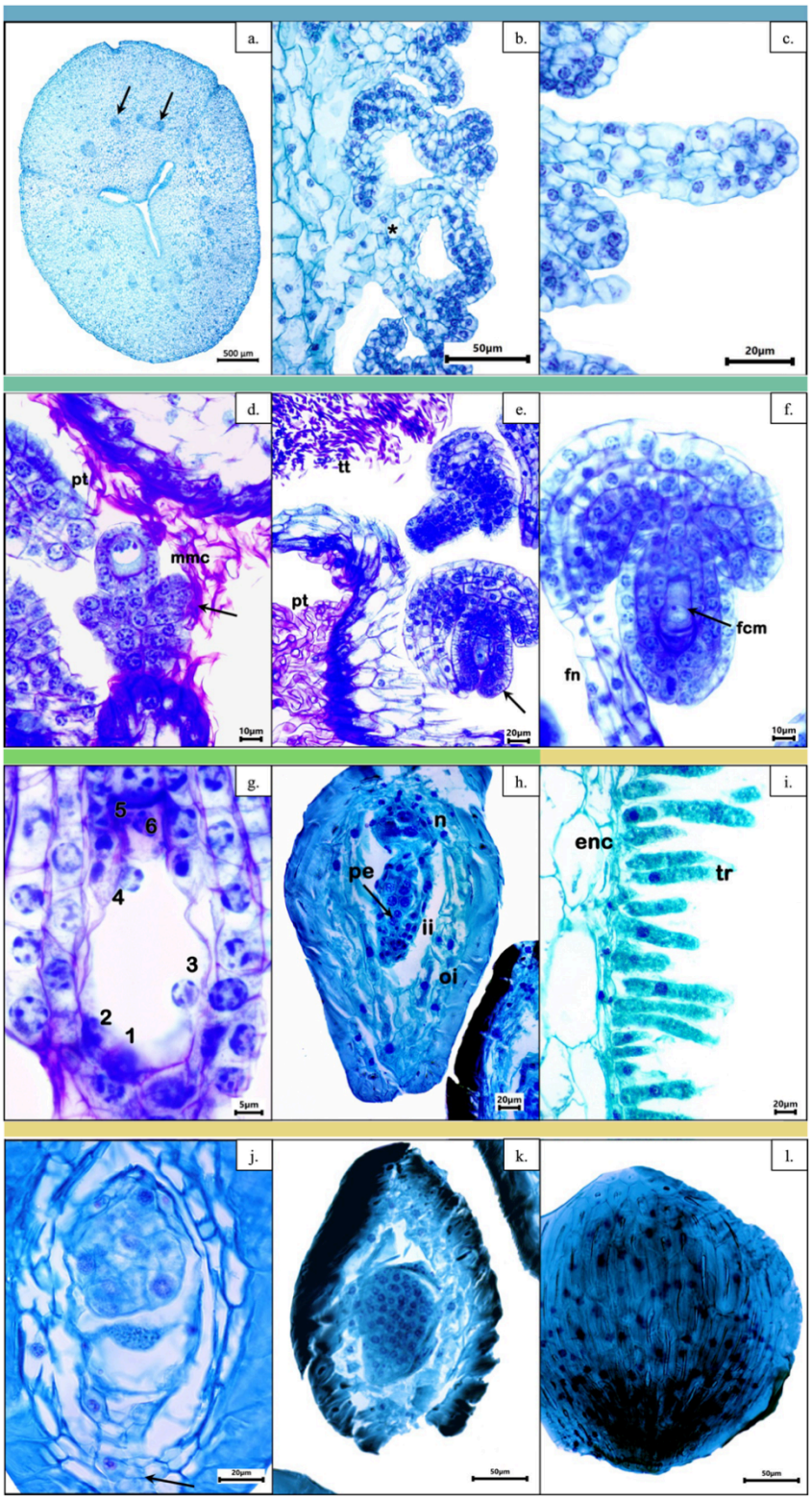


Figure 2

Anatomical ovary development during the flower-fruit transition in *Vanilla planifolia*.

Cross section of the ovary in the different stages. (**a**) Tricarpellate and unilocular ovary. Central cavity without differentiation. Vascular bundles (arrows). (**b**) Development of placental ridges in the central cavity (asterisk). (**c**) Placental projections composed of a row of cells surrounded by epidermis. (**d**)

Pollen tube (pt), young ovule with megaspore mother cell (mmc) and initiation of inner integument (arrow). (**e**) Transmitting tissue (tt), pollen tube (pt) and anatropous, bitegmic ovule (arrow). (**f**) Funiculus (fn) and elongated functional chalazal megaspore (fcm). (**g**) Mature embryo sac with six nucleus (1-6). (**h**) Developing embryo with suspensor (pe, arrow). Nucellus (n). Inner integument (ii). Developing seed coat, walls of the outermost layer of the outer integument become thickened (oi). (**i**) Unicellular trichome (tr) develops from the endocarp (enc). (**j**) Developing embryo, suspensor composed of several cells (arrow). (**k**) Globular embryo within the differentiated seed coat. (**l**) Seed coat. The color bar at the top of each image indicates the developmental stage at which each morphological change was observed: blue (Pre-pol), aqua (Pol), green (Post-pol), and yellow (Fer).

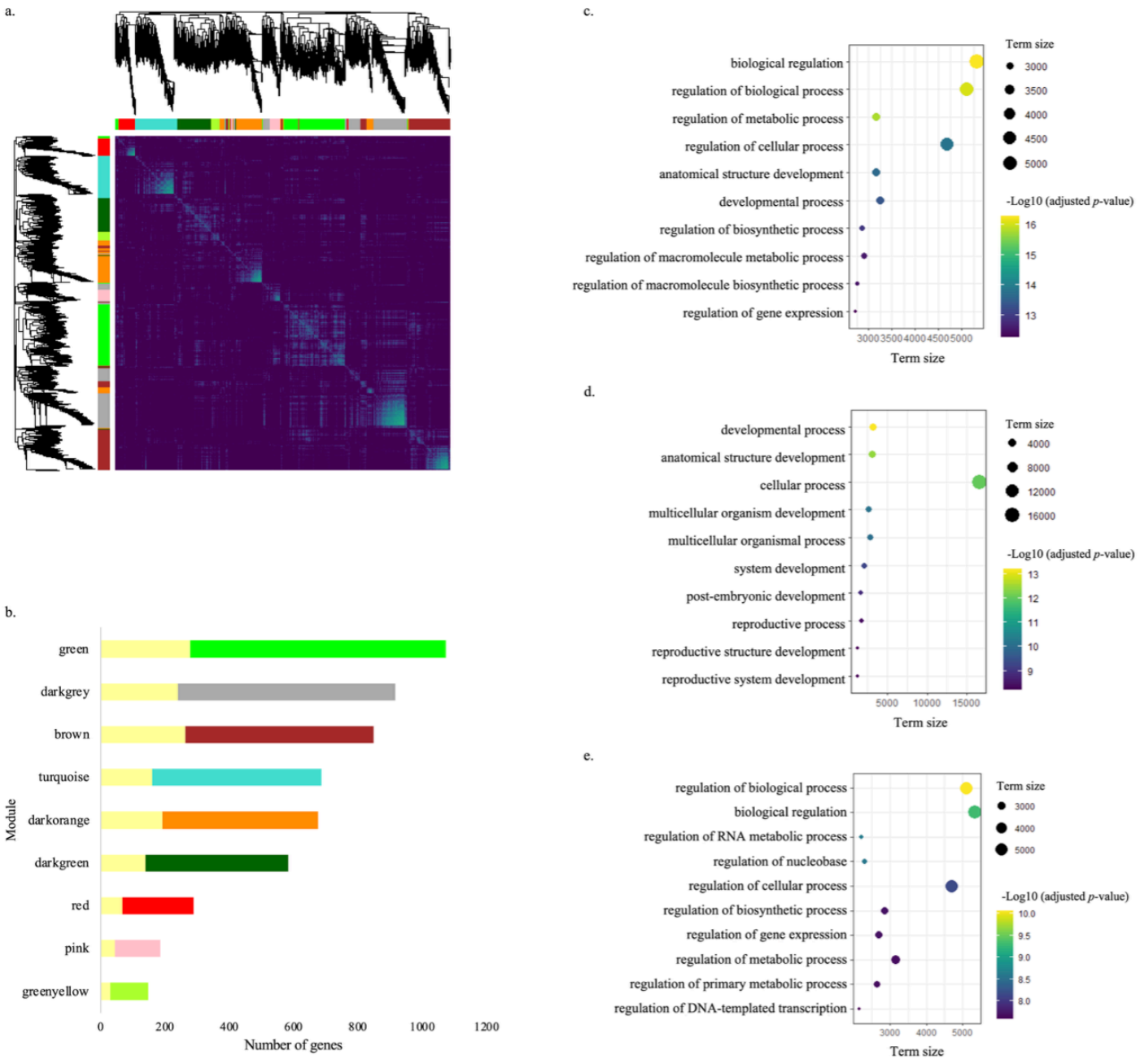


Figure 3

Network topology and functional modular organization during the flower-to fruit transition in *Vanilla planifolia*. (**a**) Heatmap of the topological overlap matrix (TOM) showing the modular structure of the global co-expression network (cut height = 0.40). (**b**) Gene distribution across modules. Bars indicate total gene counts; colored segments represent annotated genes and light yellow segments denote unannotated genes. GO biological process enrichment (gProfiler) shows the ten most significantly enriched terms per module (adjusted $p \leq 0.05$). (**c-e**)Enriched GO biological process terms for the green, dark grey and brown modules. The x-axis indicates gene counts and color gradients reflect $-\log_{10}$ (adjusted *p*-value).

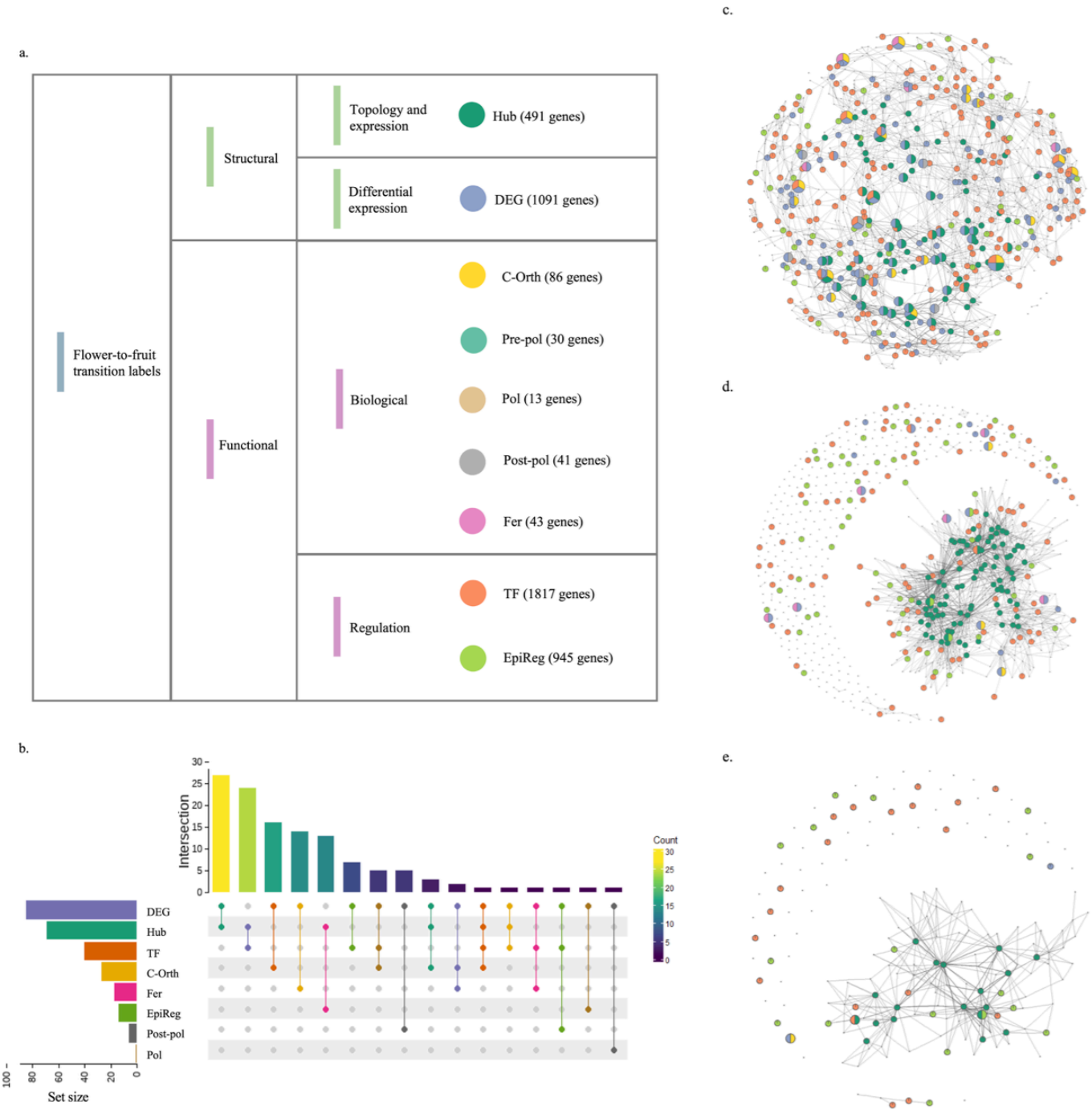


Figure 4

Co-expression module networks and multidimensional gene label intersections during the flower-to-fruit transition in *Vanilla planifolia*. (**a**) Genes were annotated using functional and structural labels. The blue bar encompasses all flower-to-fruit transition labels. Functional labels (pink bar) include conserved orthologs (C-Orth), stage-associated genes (PrePol, Pol, PostPol, and Fer), transcription factors (TFs), and epigenetic regulators (EpiReg); structural labels (green bar) include differentially expressed genes (DEGs) and module hub genes (Hubs). (**b**) Distribution of label intersections, with bars indicating gene counts and color intensity reflecting abundance. (**c–e**) Co-expression networks of the green (**c**), dark gray (**d**), and pink (**e**) modules. Nodes represent genes, edges represent co-expression relationships, pie charts show assigned label combinations, and node size reflects the number of labels.

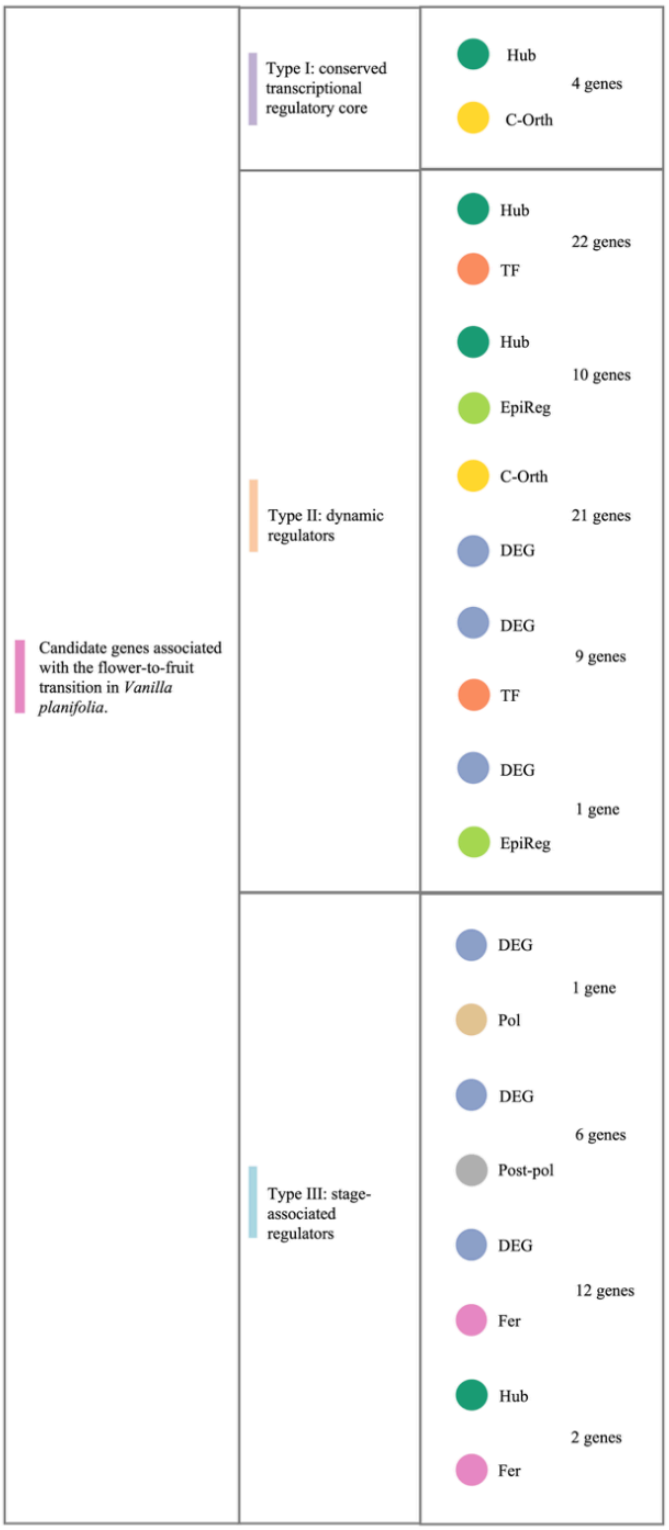


Figure 5

Candidate gene prioritization based on functional and structural labels during the flower-to-fruit transition in *Vanilla planifolia*. Genes were grouped according to combinations of functional and structural labels. The pink bar represents candidate genes associated with the flower-to-fruit transition. Colors indicate individual labels: module hub genes (Hub), differentially expressed genes (DEG), conserved orthologs (C-Orth), stage-associated genes (PrePol, Pol, PostPol, and Fer), transcription

factors (TF), and epigenetic regulators (EpiReg). Candidate genes were classified into three groups: Type I, conserved transcriptional regulatory core (purple bar); Type II, dynamic regulators (orange bar); and Type III, stage-associated regulators (blue bar).

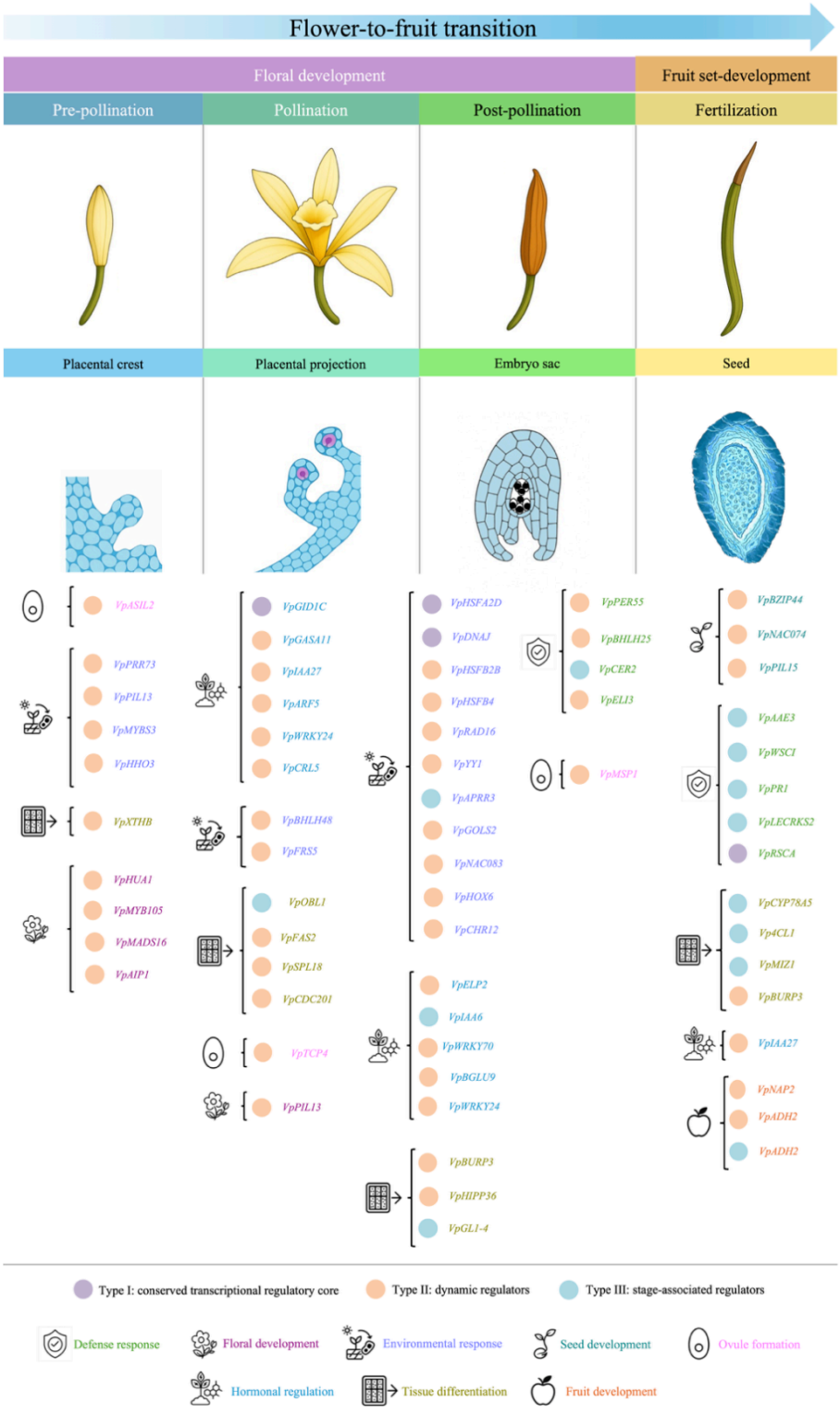


Figure 6

Integrative graphical summary of functional and structural roles of candidate genes underlying post-pollination syndrome. Conceptual model summarizing the proposed functional and structural roles of candidate genes during the FFT in *V. planifolia*, integrating anatomical evidence and network-based gene prioritization across developmental stages.

Supplementary Files

This is a list of supplementary files associated with this preprint. Click to download.

- TableS3.xlsx